



RESEARCH ARTICLE



Sapote gum as a new biopolymer suitable emulsion stabilizer: Grapeseed oil ultrasonic emulsification

Katherin Lloy Arce-Rios^{1,2} ; José Luis Pasquel-Reátegui^{1,**} ; Thony Arce-Saavedra³ ;
Eliana Marcela Vélez-Eraza^{1,*} 

¹ Grupo de Investigación en Ingeniería y Tecnología Agroindustrial, Facultad de Ingeniería Agroindustrial, Universidad Nacional de San Martín (UNSM), Tarapoto, SM, Perú.

² Department of Food Engineering, School of Food Engineering, University of Campinas, Monteiro Lobato Street, 80, 13083-862, Campinas, SP, Brazil.

³ Departamento Académico de Ciencia y Tecnología Agroindustrial, Facultad de Ciencias Agrarias, Universidad Nacional Autónoma de Chota (UNACH), Chota, Cajamarca, Perú.

* Corresponding author: elianamve@gmail.com (E. M. Vélez-Eraza).

** Corresponding author: jlpasquel@unsm.edu.pe (J. L. Pasquel-Reátegui).

Received: 19 August 2024. Accepted: 24 December 2024. Published: 14 January 2025.

Abstract

Sapote gum (SG) is a new biopolymer with promissory functional properties. This study aimed to determine if SG is a suitable emulsifier for obtaining stable grape seed oil (GSO) emulsions. In the first stage, coarse emulsion concentrations of SG and grapeseed oil - GSO were evaluated, applying the Central Composite Rotational Design (0.59% to 3.41% of SG and 12.93% to 27.07% GSO). For the second stage, using a Centered Face Design - CFD, the resulting emulsion was sonicated at 90, 270, and 450 Watts at 5, 10, and 15 min. Finally, a validation was made. Emulsions were evaluated through microstructure, droplet size, kinetic stability, heat stress, and rheology. Micrographs of the first-stage emulsions showed droplets up to 3.8 µm diameter and a creaming index between 0.00% and 28.39% after 24 h. Optimization indicates that the higher the concentration of gum (3.5%) and GSO (25%), the more kinetically stable emulsions are produced. Ultrasonic emulsions showed no significant difference in droplet size and kinetic stability before 14 days of rest. Ultrasonic validation was made at 450 W for 6 min, resulting in emulsions stable for 20 days and with rheological characteristics interesting for food or cosmetic industries.

Keywords: Central Composite Rotational Design; *Capparis scabrida*, *Vitis labrusca*; stable emulsion; Centred Face Design; ultrasound.

DOI: <https://doi.org/10.17268/sci.agropecu.2025.005>

Cite this article:

Arce-Rios, K. L., Pasquel-Reátegui, J. L., Arce-Saavedra, T., & Vélez-Eraza, E. M. (2025). Sapote gum as a new biopolymer suitable emulsion stabilizer: Grapeseed oil ultrasonic emulsification. *Scientia Agropecuaria*, 16(1), 51-59.

1. Introduction

The International Organization of Vine and Wine reported that total wine production in 2023 was 237 million hectoliters (OIV, 2024). In wine production, more than 0.2 kg of pomace is generated for every kilogram of grapes pressed, and the seeds account for 25% of this pomace (Duba & Fiori, 2015). Grapeseed oil (GSO) is a component of pomace from the wine industry. This bioproduct is important to recover because the residue from grape processing is used to do so, which helps conserve the environment and increase the added value to viticulture (Yang et al., 2021).

The GSO contains a significant amount of polyunsaturated fatty acids (PUFAs) ranging from 63.64% - 84.4% in its different grape varieties (Dabetic et

al., 2020; Fernandes et al., 2013; Górnas et al., 2018), mainly linoleic acid; It also contains isomers of vitamin E such as those found in the red Marufo grape variety, α - tocopherol (244 mg/kg of oil), γ - tocopherol (19 mg/kg of oil), α - tocotrienol (319 mg/kg of oil) and γ - tocotrienol (1575 mg/kg of oil) (Fernandes et al., 2013). This composition allows the production of high-quality functional products in order to take advantage of their properties in different presentations such as antimicrobial films (Mauro et al., 2022), biodiesel (Hazar & Sevinc, 2023), emulsions (Mutlu, 2023; Sarabandi et al., 2022), among others.

Food technology requires natural emulsions that come from sustainable and healthy production. Emulsions are generally made using high-energy

methods such as ultrasound. Nevertheless, the high-energy emulsification process as a mixing system can cause some undesirable changes in the ingredients of the food emulsion. Thus, it is essential to study the emulsion, emulsifier, and oil phase changes after sonication (Taha et al., 2020; Zhou et al., 2021). Emulsions present significant challenges that must be overcome for their application in industry. Due to emulsions being formed by two immiscible fluids in a non-spontaneous manner, they present thermodynamic instability. In addition, they have physical instabilities such as flocculation, coalescence, Ostwald ripening, phase inversion, and gravitational instabilities, characterized by an irreversible increase in the size of the dispersed phase droplets (Kelmer & Costa, 2024). Emulsifiers and stabilizers, therefore, play an important role in the food industry.

Among the biopolymers studied as GSO emulsifiers are milk protein (Sarabandi et al., 2022; Silva et al., 2020a), gelatin/sodium alginate (Mutlu, 2023), gum arabic (Surini et al., 2018), lupine Protein (Francisco et al., 2023), poppy pollen protein and peptides (Sarabandi et al., 2023), polyglycerol polyglycinate polyglycinate /whey protein isolate with konjac glucomannan (Zhuang et al., 2023), pectin/gelatin (Khah et al., 2021). However, no further information exists on the use of sapote gum as a stabilizer or emulsifier. Previous studies have reported that its use as a coating on bananas was promising; it was able to preserve the fruit's characteristics over the storage period (Vélez-Erazo et al., 2022). In addition, as a plasticizer in chitosan films, it has better properties than other natural plasticizers (Gonzaga et al., 2019).

Capparis scabrida is a tree grown in Peru, Ecuador, Venezuela, Colombia, Bolivia, Panama, Brazil, and Costa Rica, from which the gum is extracted from vascular exudations (Herz Castro, 2007). The use of this species is mainly forestry due to the value of its wood, and its deforestation has led the Peruvian government to declare the species in critical danger of extinction and scientists to promote conservation strategies (Abreu-Naranjo et al., 2020; Rodríguez-Rodríguez et al., 2007). The gum has a moisture content of 11% to 12%, water solubility value of 91% to 98%, viscosity of 230 cps at 17%, pH of 4.41 (Herz Castro, 2007), and high in protein (8.45% - 9.3%) and carbohydrates content (83.5% - 86.46%) (Herz Castro, 2007; Moscol Ortiz, 2018). Thus, its application as a stabilizer represents an interesting alternative due to its biodegradable presentation compared to synthetic polymers and toxic preservatives.

For all the above, the objective of this research was to study, for the first time, the sapote gum potential to form and stabilize grapeseed oil emulsion using ultrasound as an emulsion-forming technique.

2. Methodology

Material

Grape seed oil (*Vitis labrusca*) was purchased by the company Nature, located in the province of San Martín, department of San Martín, Peru, which uses burgundy grape seeds from the viticulture of local producers. The oil was kept refrigerated until use. The sapote gum (*Capparis scabrida*) (protein (8.45% - 9.3%) and carbohydrate content (83.5% - 86.46%) (Herz Castro, 2007; Moscol Ortiz, 2018)) was provided by local producers in the Almirante Miguel Grau, located in Piura, Peru.

Obtention of pre-emulsion

The sapote gum and water solution were left in magnetic stirring for 24 h, then GSO was added. An Ultraturrax rotor-stator (Ika, Werke GmbH and Co. KG, Staufenim Breisgau, Germany) was used to form the emulsion by stirring at 12000 rpm for 2 minutes, and the emulsion was immediately analyzed by optical microscopy and kinetic stability for 24 hours. The different proportions of sapote gum and GSO were combined according to the Central Composite Rotational Design (CCRD) type design between 0.59% and 3.41%, and 12.93% and 27.07%, respectively (Table 1).

Obtention of ultrasonic-emulsion

The optimal emulsion of the previous assay was subjected to ultrasound (900W full power, 20 kHz frequency, Branson 250, USA, probe ($\varnothing = 12.5$ mm)) at different conditions of power amplitude (10%, 30% and 50%), which provided nominal powers of 90, 270, and 450 Watts, respectively; and time (5, 10, and 15 min) according to the Centred Face Design (CFD) generating 12 treatments (Table 2). The ultrasonic emulsion was immediately analyzed by optical microscopy and kinetic stability for 0, 7, and 14 days (the emulsion was kept under laboratory conditions until the analysis was performed).

Characterization of pre-emulsion and ultrasonic emulsion

Kinetic stability

For the analysis of kinetic stability, we proceeded according to Vélez-Erazo et al. (2018), where 40 mL of each previous emulsion was placed in 100 mL graduated tubes and then left in ambient conditions for 24 hours. Phase formation was then observed,

and the oil phase volume was recorded every 30 minutes for the first 3 hours and at 24 hours. The details of the kinetic stability analysis are shown in Figure 1.

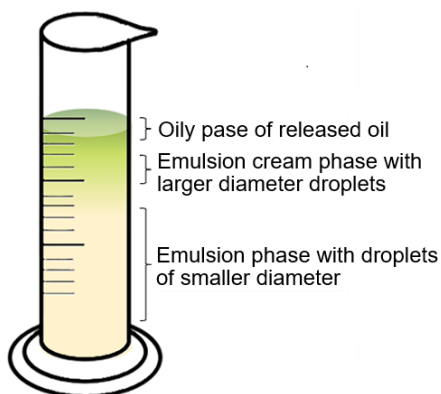


Figure 1. Phases observed in kinetic stability analysis.

The kinetic stability was calculated according to the oil release (OR), creaming index (CI), and Creaming - Oil index (COI) given in equations 1, 2, and 3 which is defined between the ratio of the height of the oil phase, creaming phase or creaming-oil phase of the emulsion (H) and the initial height (Ho).

$$\%OR = \left(\frac{H_{oil}}{H_o}\right) \times 100 \quad (\text{Eq 1})$$

$$\%CI = \left(\frac{H_{creaming}}{H_o}\right) \times 100 \quad (\text{Eq 2})$$

$$\%COI = \left(\frac{H_{creaming+oil}}{H_o}\right) \times 100 \quad (\text{Eq 3})$$

Where Ho represents the initial volume of the emulsion, and H is the volume of the upper or cream phase. The CI was determined in duplicate, and the results were expressed as mean ± standard deviation.

For the analysis of the kinetic stability of the ultrasonic emulsion, 25 mL of each treatment was placed in graduated specimens of 50 mL, where the emulsions were analyzed on days 0, 7, and 14; in addition, for this last day, the ultrasonic emulsions were subjected to thermal stress in a water bath at 90 °C for 20 minutes, following the methodology of Li et al. (2023).

Optical microscopy and droplet diameter

It was determined by optical microscopy using a microscope (Nikon, Eclipse Ni-U model) with an amplitude of 40x (previous emulsions) and 100x with immersion oil (ultrasonic emulsions), with image capture through the digital camera controlled by the Motic Images Plus program. For the analysis of the micrographs, the ImageJ software was used, which allowed for determining the area of the droplets (400 drops/treatment) and, from this, calculated the theoretical average diameter according to equation 4 according to Saout et al. (1999).

$$\text{Theoretical diameter} = \sqrt{\frac{4 \times \text{AREA}}{\pi}} \quad (\text{Eq 4})$$

Table 1
Central Composite Rotational Design (CCRD) and characteristics of pre-emulsions

Exp	Gum (%)	Oil (%)	Oil release	Creaming index	Creaming - Oil index	Diameter (µm)
1	-1(1)	-1(15)	7.14±0.91	9.74±0.92	16.88±0.00	4.94±3.10
2	1(3)	-1(15)	0.00±0.00	8.11±0.00	8.11±0.00	3.79±2.75
3	-1(1)	1(25)	6.58±1.86	14.47±1.86	21.05±0.00	4.72±4.07
4	1(3)	1(25)	0.00±0.00	0.00±0.00	0.00±0.00	4.51±2.09
5	-1.41(0.59)	0(20)	15.07±0.00	9.59±0.00	24.66±0.00	4.90±2.44
6	1.41(3.41)	0(20)	0.00±0.00	1.35±0.00	2.01±0.93	3.98±1.87
7	0(2)	-1.41(12.93)	2.67±0.05	10.67±0.20	13.34±0.25	4.11±2.00
8	0(2)	1.41(27.07)	2.58±0.02	28.39±0.26	30.97±0.28	4.87±3.03
9	0(2)	0(20)	3.21±0.97	13.46±0.66	16.67±0.30	5.33±3.53
10	0(2)	0(20)	3.21±0.97	13.46±0.66	16.67±0.30	4.97±3.06
11	0(2)	0(20)	3.20±0.85	12.82±0.23	16.02±0.61	5.00±3.18
12	0(2)	0(20)	2.58±0.02	14.19±0.13	16.77±0.15	4.24±2.31

Table 2
Central Face Design (CFD) and Particle Diameter (µm)

T	X ₁ (Watts)	X ₂ (Min)	D0	D7	D14	WB
1	-1 (90)	-1 (5)	1.60±0.73	2.37±1.18	2.05±0.81	1.80±0.87
2	1 (450)	-1(5)	1.90±0.69	1.86±1.07	1.55±0.61	1.61±0.39
3	-1(90)	1(15)	2.10±0.92	1.75±0.90	1.49±0.51	1.41±0.35
4	1(450)	1(15)	2.09±0.49	1.73±0.64	1.42±0.60	1.85±0.54
5	-1(90)	0(10)	1.82±0.76	1.30±0.47	1.54±0.56	1.36±0.35
6	1(450)	0(10)	1.84±0.59	1.64±0.62	1.36±0.47	2.00±0.93
7	0(270)	-1(5)	1.81±0.71	1.64±0.60	1.69±0.50	1.59±0.37
8	0(270)	1(15)	1.65±0.71	1.82±0.74	1.25±0.32	1.70±0.40
9	0(270)	0(10)	1.42±0.58	1.92±0.82	1.73±0.44	1.63±0.50
10	0(270)	0(10)	2.04±0.78	1.59±0.52	1.65±0.48	1.79±0.56
11	0(270)	0(10)	1.61±0.711	1.24±0.45	1.58±0.43	1.53±0.34
12	0(270)	0(10)	1.77±0.59	1.56±0.82	1.49±0.35	1.82±0.70

D0: particle diameter day 0, D7: particle diameter day 7, D14: particle diameter day 14, and WB: particle diameter after water bath (heat stress).

Validation

A validation experiment was carried out by preparing a pre-emulsion at 3.5% SG and 25% GSO using an Ultraturrax rotor-stator (Ika, Werke GmbH and Co. KG, Staufenim Breisgau, Germany) at 12000 rpm for 2 minutes. Finally, an ultrasonic emulsion was obtained at 450W by 6 min (Branson 250, USA, probe ($\varnothing = 12.5$ mm)).

The emulsion was characterized according to kinetic stability using a Turbiscan LAB® basic (Formulation, L'Union, France) at days 0, 3, 6, 10, 12, 17, and 20. Rheological assays were made using a rheometer (Anton Paar MCR 302, GmbH, Graz, Austria) equipped with a 40 mm flat plate geometry and a gap of 1000 μm . Flow curves were obtained at a shear rate of 1–300 s^{-1} (up, down, up), and results were adjusted to the Herschel-Bulkley (HB) model ($\sigma = \sigma_0 + k \cdot \dot{\gamma}^n$). Amplitude (Strain 0.01-100% at 1Hz) and angular frequency (1–100 rad/s at strain 0.1) sweep were carried out for viscoelastic parameters. Finally, thixotropy assays were developed in three intervals, first and third intervals at 1 s^{-1} for 400 s, and the second interval at 80 s^{-1} for 200 s. All rheological assays were made at 25 °C (Medeiros et al., 2022).

Statistical analysis

A Central Composite Rotational Design (CCRD) was applied to characterize the previous emulsion in the homogenizer at $p \leq 0.05$. A Centred Face Design (CFD) with a $p \leq 0.10$ was used for the ultrasonic emulsion. Protimiza software was used in both

analyses to determine the mathematical model that best fits the experimental results. The statistical analysis allowed us to identify the effects of the variables and their interaction on the responses of oil release, cream index, and droplet size.

3. Results and discussion

Characterization of the pre-emulsion

The characterization of the pre-emulsion (Table 1 and Figure 2) was performed to determine the optimal concentration of GSO and sapote gum of a stable emulsion capable of retaining the greatest amount of oil with the least amount of sapote gum. The relationship between kinetic stability and droplet size compromises the quality of the emulsion. Thus, after emulsion preparation, T2, T4, and T6 resulted in uniform and homogeneous emulsion, treatments with the highest concentrations of sapote gum used (3% and 3.41%, respectively) (Table 1). During the 24 hours observed, T2 and T6 had a cream phase with no oil release, and only the T4 did not present a cream phase or oil release (Figure 2). In relation to droplet size, the diameter fluctuated between 3.79 μm (T2) and 5.33 μm (T9), and all samples presented similar microstructure and droplet size distribution (Figure 2). The ANOVA finds that gum concentration has a significant effect (P-value equal to 0.031), which is explained in the mathematical model that the higher the gum concentration, the smaller the particle size. This difference is visibly unobservable.

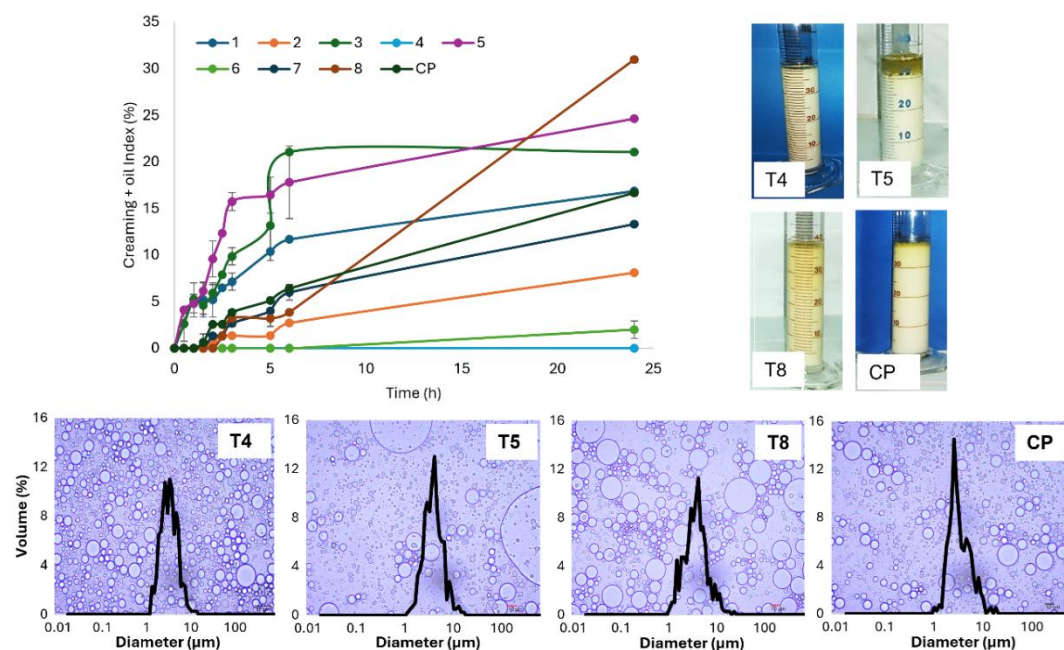


Figure 2. Pre-emulsion characterization. Creaming + oil index kinetic and macrostructure at 24 h (up), and microstructure and droplet size distribution of T4, T5, T8 and central point (CP) (Down).

Figure 3 shows the trend areas according to the statistical methodology applied. Figure 3A shows that axial oil concentrations (12,93% and 27.07%) do not significantly affect oil release. In contrast, when the gum concentration is < 2%, the emulsion results in oil release. This behavior demonstrates the influence of gum concentration on the emulsion on oil release. Figures 3B and C show that, at sapote gum concentrations less than 3.25% with high oil concentration, the greater the formation of the creaming phase, and when the concentration of gum is ≥ 3.25%, regardless of the oil concentration, the emulsion results in less formation of the creaming phase. Figure 3D shows that the lower the oil concentration (<14%) and the higher the gum concentration (> 3.25%), the smaller the droplet size.

Table 3
Reparameterized model for Oil Release, Creaming Index, Creaming Oil Index, and Droplet Size of Pre-emulsions

Variable response	Polynomial Equations	R ² (%)
Oil Release	$Y_1 = 3.05 - 4.38 x_1 + 1.83 x_1^2 - 0.63 x_2^2$	93.26
Creaming Index	$Y_2 = 15.02 - 3.47 x_1 - 5.50 x_1^2 + 2.71 x_2 - 3.21 x_1 x_2$	70.40
Creaming Oil Index	$Y_3 = 17.53 - 7.73 x_1 - 3.41 x_1^2 + 2.62 x_2 - 3.07 x_1 x_2$	77.07
Droplet Size	$Y_4 = 4.88 - 0.33 x_1 - 0.22 x_1^2 + 0.20 x_2 + 0.19 x_2^2 + 0.24 x_1 x_2$	73.27

Table 3 presents the reparameterized model for each response variable, considering the significance of the factors in descending order. This reparameterized

model allowed us to find the equation that represents the optimization of sapote gum and oil concentrations based on an acceptable R². Finally, the generated models explain the experimental results much more about the release of oil (R² = 93.26%). These results are corroborated by the p-value, which was less than 0.05 for most means.

All response variables (oil release, creaming index, creaming-oil index, and droplet size) of the previous emulsion were adjusted to second-order polynomial equations, where it is observed that the effect of sapote gum concentrations (X₁) is significant compared to GSO concentrations (X₂). These equations demonstrate the stabilizing capacity of sapote gum since as the gum concentration (X₁) increases, the cream formation and the oil release tend to decrease. Notwithstanding, as the GSO (X₂) increases, the formation of cream tends to increase. The effects of droplet size are opposite since as X₁ and X₂ concentrations increase, droplet size tends to decrease and increase, respectively, represented by negative and positive signs in the coefficients (Table 3).

All this is explained by the fact that by increasing the gum and decreasing the oil that the surface of the droplets formed, they are covered by the protein in its entirety, ensuring emulsification. Furthermore, the polysaccharides in the gum fulfill a steric function by increasing the viscosity of the emulsion and preventing the formed droplets from moving and interacting with each other (Vélez-Erazo et al., 2020).

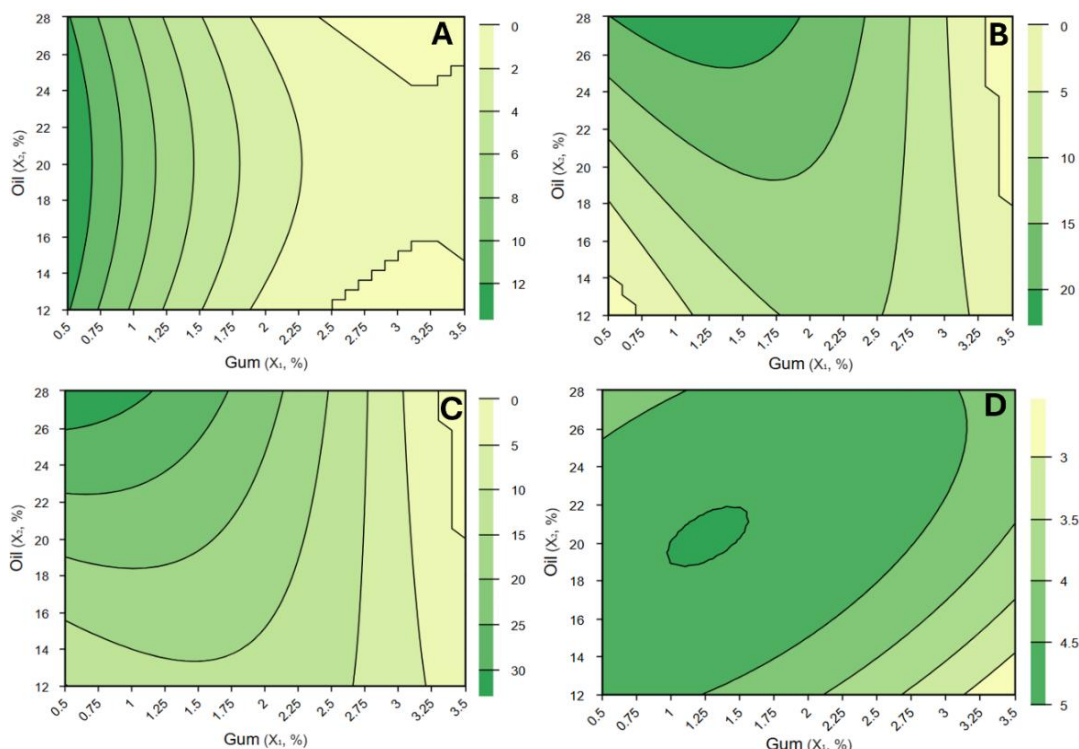


Figure 3. Pre-emulsion Contour Plot for Oil Release (A), Creaming Index (B) Creaming-Oil Index (C), and Droplet Size (D).

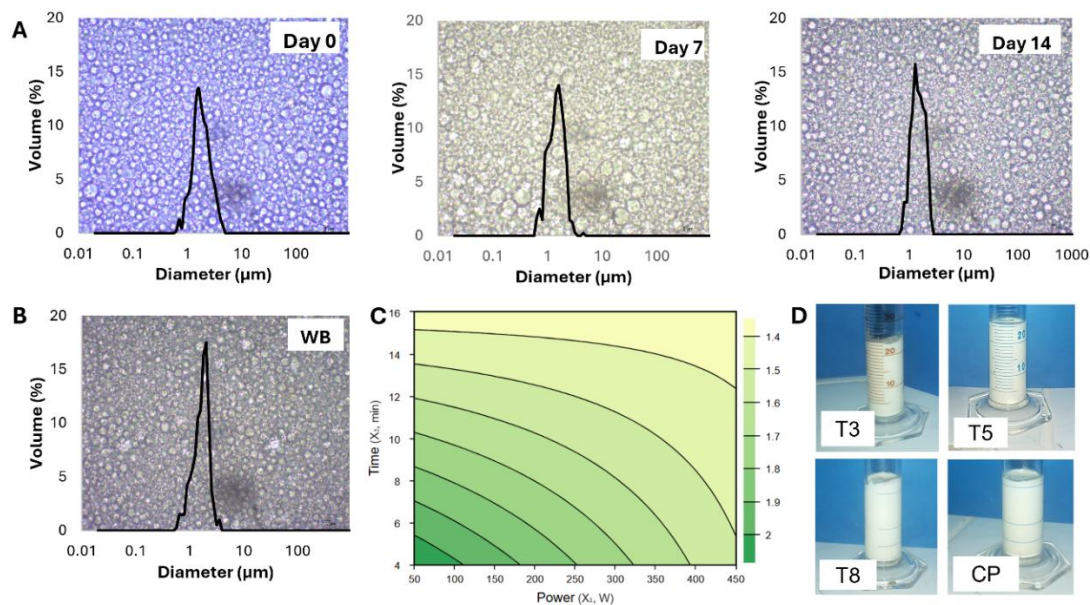


Figure 4. Ultrasound-emulsion characterization. microstructure and droplet size distribution of central point at days 0, 7, 14 (A), and after water bath (heat stress) (B), Droplet diameter contour chart at day 14 (C), and Macrostructure at day 14 (D).

Similar results were obtained by [Sepeidnameh et al. \(2024\)](#). The authors analyzed the stability of GSO-multilayer emulsions stabilized by gelatin, gelatin-chitosan, and gelatin-chitosan-basil seed gum homogenized only by a rotor-stator device. All emulsions presented phase separation at day 7, reaching values of 36%, 46%, and 53% of the creaming index for emulsions stabilized by gelatin, gelatin-chitosan, and gelatin-chitosan-basil seed gum, respectively.

Characterization of ultrasonic emulsion

The purpose of using a Centred Face Design (CFD) was to establish the optimal ultrasonic power and time application conditions for the formation of stable emulsions using optimized pre-emulsion of sapote gum (3.50%) and GSO (25%). These concentrations were defined by analyzing [Figure 3](#), with the aim to obtain less oil release ([Figure 3A](#)), less cream formation ([Figure 3B](#) and [C](#)), and the smallest droplet size ([Figure 3D](#)). These responses were analyzed to determine the greatest possible GSO incorporation. In response to this step, the ultrasound-emulsion characterization is presented in [Figure 4](#) and [Table 2](#).

As shown in [Figure 4](#), the ultrasonic emulsions presented similar microstructure and monomodal droplet size distribution. Also, these emulsions did not exhibit creaming phase formation, indicating that the emulsions had good kinetic stability during the evaluation period (14 days), even after heat stress. Results coincided with the study of [Silva et al. \(2015\)](#) on ultrasound's effectiveness in producing kinetically stable single or double emulsions ([Li et al., 2023](#)).

In some treatments, the development of dark-colored colonies was observed on day 7, possibly due to the presence of microorganisms, which could cause the collapse of interfacial protein structure, the oxidation of lipids, and finally, the destabilization of the emulsion ([Yuan et al., 2013](#)). However, in this case, their presence on the emulsions until day 14 did not signify an instability factor. Given the good stability of this emulsion, it is recommended that antimicrobials be used for future work.

In relation to particle size, it is observed that on day 0, the diameter varies between 1.418 μm and 2.092 μm, on day 7 between 1.239 μm and 2.369 μm, on day 14 between 1.251 μm and 2.054 μm, and after heat stress between 1.359 μm and 1.998 μm ([Table 2](#)).

Statistical results reveal that on days 0 and 7, there were no significant effects of variables (power and sonication time) on droplet size due to the low R^2 observed ([Table 4](#)). The droplet size was so homogeneous that no difference was observed when applying a statistical analysis, which does not necessarily mean something negative. In contrast, after 14 days, the sonication time variable appears to be a slightly influential factor in droplet size and a higher degree of correlation with droplet diameter. This behavior implies that the longer the emulsion rest time, the more the droplet structure is re-shaped. Similar studies suggest optimal conditions for producing 10-day stable sonoemulsions at GSO (10% w/w) and protein solutions (3.3% w/w) with casein:whey protein ratios of 60:40, 50:50, 40:60 produced with an energy density of 81.9 J mL⁻¹ (500

W at 60% amplitude for 7 minutes) (Silva et al., 2019, 2020a).

Table 4

Reparametrized model for ultrasound-emulsion' droplet size

Diameter	Polynomial Equations	R ²
Day 0	$Y_1 = 1.70 + 0.06 x_1 + 0.16 x_1^2 + 0.09 x_2 + 0.05 x_2^2 - 0.07 x_1 x_2$	38.30
Day 7	$Y_2 = 1.53 - 0.03 x_1 + 0.05 x_1^2 - 0.09 x_2 + 0.30 x_2^2 + 0.12 x_1 x_2$	45.09
Day 14	$Y_3 = 1.56 - 0.13 x_1 - 0.18 x_2 + 0.11 x_1 x_2$	73.38

The results of the droplet diameter of the emulsion after 14 days of resting show that there is a significant difference between the treatments and, in the contour graph (Figure 4C), the tendency is observed that the longer the time and power of sonication, the smaller the particles are formed. These results express a polynomial equation based on a correlation greater than 70%. Before 14 days, it was not possible to define a mathematical model that would respond to the optimization of the process because the warhead did not compromise the two variables.

Silva et al. (2020b) obtained GSO-ultrasound emulsions stabilized with milk proteins. The authors found that ultrasound can form small droplets (<3 μm), which is related to high emulsion stability. These results are similar to those found in the present study, highlighting the potential of sapote gum to form and stabilize GSO emulsions since sapote gum presented an emulsifying behavior similar to an excellent emulsifier such as milk proteins.

Validation

A final validation experiment was made after variable analyses. As all emulsions were stable for 14 days

(without phase separation), ultrasound parameters were determined at 450 W for 6 min, calculating a droplet size < 1.5 μm (Figure 4C). At these conditions, low process time and high potency avoid overprocessing (increasing the temperature) and allow work at low energy density, reducing the energy cost (Vélez-Erao et al., 2018). Results show that the final assay is stable for 20 days without phase separation or another destabilization process (Figure 5A).

Figure 5B-F shows the rheological characterization. Several models are widely used for fitting experimental flow data, such as Ostwald, Casson, Mizarhi-Berk, and Herschel Buckley (Gamboa-Alarcón et al., 2023). Experimental data presented a good adjustment to the Herschel-Bulkley model (R²>0.99) and showed a shear-thinning behavior due to the flow behavior index (n) being a little higher than 1 (1.19). Additionally, apparent viscosity decreases as the shear rate increases.

On the other hand, in oscillatory assays, loss modulus (G'') was higher than storage modulus (G'), indicating that emulsion was predominantly viscous material affected mainly by frequency. Figure 5E demonstrates that SG-emulsion is also characterized as a concentrated solution without gel behavior despite showing a clear tendency for elastic-like behavior at higher frequencies (Steffe, 1996).

Finally, the thixotropy test evaluates the deformation and regenerative capacity of the emulsion, presenting a recovery percentage of 73% (Calculated as the relation of the final viscosity of the first interval and the first viscosity of the third interval). An acceptable recovery percentage (over 70%) was obtained, suggesting that this emulsion can be used in systems requiring reversible deformation (Wu et al., 2022).

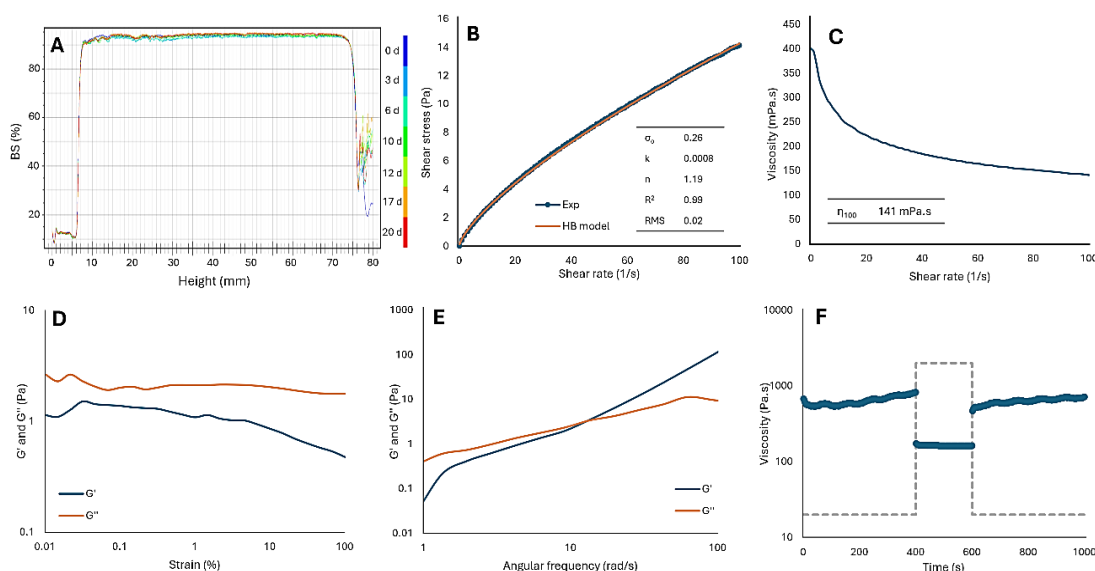


Figure 5. Validation experiment characterization. Backscattering profile (A), Shear stress (B), viscosity (C), Amplitude (D), frequency (E) and Thixotropy curves (F).

4. Conclusions

Sapote gum (*Capparis scabrida*) is a new biopolymer that demonstrated emulsifying capacity, maintaining grapeseed oil-emulsion stability during the evaluated time (20 days). Two experimental designs were established using response surface methodology to study the variables' modeling and the optimal values for formulation (rotor-stator pre-emulsions) and ultrasonic parameters (Ultrasonic emulsions).

In the rotor-stator pre-emulsions, some experiments presented phase separation after a few hours of storage, and droplet size varied between 3.79 and 5.33 μm . The optimized pre-emulsion was defined as 3.5% sapote gum and 25% grapeseed oil. Ultrasonic emulsions did not present phase separation during 14 days of storage, even after heat treatment. Ultrasound decreases the droplet size (1.25 – 2.37 μm), ensuring emulsion stability.

Finally, an emulsion' validation was made with 3.5% sapote gum and 25% grapeseed oil and with ultrasonic parameters of 450 W for 6 min. This emulsion resulted in a shear-thinning fluid with predominantly viscous behavior, being a concentrated solution without gel behavior and with reversible deformation. All these characteristics allow the incorporation of sapote gum-stabilized emulsion in a wide range of products.

Future investigations are necessary because there are no studies on the application of sapote gum as a biopolymer in different industries, such as food, cosmetics, or pharmaceuticals.

Author's contribution

K. L. Arce-Rios: Conceptualization, Methodology, Formal Analysis, Visualization, Writing - Review & Editing Original Draft. **J. L. Pasquel Reátegui:** Supervision, Conceptualization, Project administration, Funding acquisition, Writing – Review & Editing. **T. Arce-Saavedra:** Writing - Review & Editing Original Draft. **E. M. Vélez-Erazo:** Supervision, Conceptualization, Writing - Review & Editing.

Funding Declaration

This study was financially supported by Instituto de Investigación (IDI-UNSM-PERÚ) Resolución N° 623-2022-UNSM/CU-R.




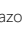
Data Availability

The authors confirm that the data supporting the findings of this study are available within the article.

Declarations of Conflict of Interest

The authors declare no competing interests.

ORCID

K. L. Arce-Rios  <https://orcid.org/0000-0003-1933-9533>
 J. L. Pasquel-Reátegui  <https://orcid.org/0000-0001-6467-394X>
 T. Arce-Saavedra  <https://orcid.org/0000-0002-2300-9169>
 E. M. Vélez-Erazo  <https://orcid.org/0000-0002-8632-5329>

References

- Abreu-Naranjo, R., Ramirez-Huila, W. N., Reyes Mera, J. J., Banguera, D. V., & León-Camacho, M. (2020). Physico-chemical characterisation of *Capparis scabrida* seed oil and pulp, a potential source of eicosapentaenoic acid. *Food Bioscience*, *36*, 100624. <https://doi.org/10.1016/J.FBIO.2020.100624>
- Dabetic, N. M., Todorovic, V. M., Djuricic, I. D., Stankovic, J. A. A., Basic, Z. N., Vujovic, D. S., & Sobajic, S. S. (2020). Grape Seed Oil Characterization: A Novel Approach for Oil Quality Assessment. *European Journal of Lipid Science and Technology*, *1900447*, 1–10. <https://doi.org/10.1002/ejlt.201900447>
- Duba, K. S., & Fiori, L. (2015). Supercritical CO₂ extraction of grape seed oil: Effect of process parameters on the extraction kinetics. *The Journal of Supercritical Fluids*, *98*, 33–43. <https://doi.org/10.1016/J.SUPFLU.2014.12.021>
- Fernandes, L., Casal, S., Cruz, R., Pereira, J. A., & Ramalhosa, E. (2013). Seed oils of ten traditional Portuguese grape varieties with interesting chemical and antioxidant properties. *Food Research International*, *50*(1), 161–166. <https://doi.org/10.1016/j.foodres.2012.09.039>
- Francisco, C. R. L., Santos, T. P., & Cunha, R. L. (2023). Nano and micro lupin protein-grape seed extract conjugates stabilizing oil-in-water emulsions. *Food Hydrocolloids*, *135*, 108117. <https://doi.org/10.1016/J.FOODHYD.2022.108117>
- Gamboa-Alarcón, P. W., Enriquez-Castillo, D. F., Suyón-Martínez, J. A., & Rodríguez-Paúcar, G. N. (2023). Comportamiento reológico de la pulpa de mango (*Mangifera indica* L.) liofilizada con encapsulantes. *Revista Agrotecnológica Amazónica*, *3*(1), e436. <https://doi.org/10.51252/raa.v3i1.436>
- Gonzaga, A., Rimaycuna, J., Cruz, G. J. F., Bravo, N., Gómez, M. M., Solís, J. L., & Santiago, J. (2019). Influence of natural plasticizers derived from forestry biomass on shrimp husk chitosan films. *Journal of Physics: Conference Series*, *1173*(1). <https://doi.org/10.1088/1742-6596/1173/1/012006>
- Górnaś, P., Rudzińska, M., Grygier, A., & Łációs, G. (2018). Diversity of oil yield, fatty acids, tocopherols, tocotrienols, and sterols in the seeds of 19 interspecific grapes crosses. *Journal of the Science of Food and Agriculture*, *99*(5), 2078–2087. <https://doi.org/10.1002/J.SFA.9400>
- Hazar, H., & Sevinc, H. (2023). Investigation of exhaust emissions and performance of a diesel engine fueled with preheated raw grape seed oil/propanol blends. *Chemical Engineering and Processing - Process Intensification*, *188*, 109378. <https://doi.org/10.1016/J.CEP.2023.109378>
- Herz Castro, K. B. (2007). Análisis físico-químico de la goma exudada de la especie sapote (*Capparis scabrida* H.B.K.), proveniente de los bosques secos de Lambayeque. In *Universidad Nacional Agraria La Molina*. <http://repositorio.lamolina.edu.pe/handle/20.500.12996/403>
- Kelmer, F., & Costa, F. F. (2024). Innovations and stability challenges in food emulsions. *Sustainable Food Technology*. <https://doi.org/10.1039/D4FB00201F>
- Khah, M. D., Ghanbarzadeh, B., Roufegarinejad Nezhad, L., & Ostadrahimi, A. (2021). Effects of virgin olive oil and grape seed oil on physicochemical and antimicrobial properties of pectin-gelatin blend emulsified films. *International Journal of Biological Macromolecules*, *171*, 262–274. <https://doi.org/10.1016/J.IJBIOMAC.2021.01.020>
- Li, J., Wang, S., Wang, H., Cao, W., Lin, H., et al. (2023). Effect of ultrasonic power on the stability of low-molecular-weight oyster peptides functional-nutrition W1/O/W2 double emulsion. *Ultrasonics Sonochemistry*, *92*, 106282. <https://doi.org/10.1016/j.ultsonch.2022.106282>
- Mauro, M., Pinto, P., Settanni, L., Puccio, V., Vazzana, M., Hornsby, B. L., et al. (2022). Chitosan Film Functionalized with Grape Seed Oil—Preliminary Evaluation of Antimicrobial Activity.

- Sustainability*, 14(9), 5410. <https://doi.org/10.3390/SU14095410>
- Medeiros, A. M., Vélez-Eraza, E. M., Grossi, G., Furtado, G. D. F., Vidotto, D. C., Tavares, G. M., & Hubinger, M. D. (2022). High internal phase emulsions stabilized by the lentil protein isolate (*Lens culinaris*). *Colloids and Surfaces A: Physicochemical and Engineering Aspects*, 653(June), 129993. <https://doi.org/10.1016/j.colsurfa.2022.129993>
- Moscol Ortiz, J. A. (2018). *Caracterización física-química para determinación del rendimiento y calidad de la goma exudada de la especie forestal sapote Capparis scabrida H.B.K en el área de conservación regional angostura faical*. Universidad Nacional de Tumbes.
- Mutlu, N. (2023). Effects of grape seed oil nanoemulsion on physicochemical and antibacterial properties of gelatin-sodium alginate film blends. *International Journal of Biological Macromolecules*, 237, 124207. <https://doi.org/10.1016/j.IJBIOMAC.2023.124207>
- OIV. (2024). *State of the world vine and wine sector in 2023*.
- Rodríguez-Rodríguez, E. F., Bussmann, R. W., Jackeline, S., Alfaro, A., & López, E. (2007). *Capparis scabrida (Capparaceae) una especie del Perú y Ecuador que necesita planes de conservación urgente Capparis scabrida (Capparaceae) a species from Peru and Ecuador in urgent*. <https://www.researchgate.net/publication/228108008>
- Saout, C., Quéré, C., Donval, A., Paulet, Y. M., & Samain, J. F. (1999). An experimental study of the combined effects of temperature and photoperiod on reproductive physiology of *Pecten maximus* from the Bay of Brest (France). *Aquaculture*, 172(3–4), 301–314. [https://doi.org/10.1016/S0044-8486\(98\)00406-2](https://doi.org/10.1016/S0044-8486(98)00406-2)
- Sarabandi, K., Akbarbaglu, Z., Mazloomi, N., Gharehbeglou, P., Peighambaroust, S. H., & Jafari, S. M. (2023). Structural modification of poppy-pollen protein as a natural antioxidant, emulsifier and carrier in spray-drying of O/W-emulsion: Physicochemical and oxidative stabilization. *International Journal of Biological Macromolecules*, 250, 126260. <https://doi.org/10.1016/j.ijbiomac.2023.126260>
- Sarabandi, K., Tamjidi, F., Akbarbaglu, Z., Samborska, K., Gharehbeglou, P., Kharazmi, M. S., & Jafari, S. M. (2022). Modification of Whey Proteins by Sonication and Hydrolysis for the Emulsification and Spray Drying Encapsulation of Grape Seed Oil. *Pharmaceutics*, 14(11), 2434. <https://doi.org/10.3390/PHARMACEUTICS14112434/S1>
- Sepeidnameh, M., Fazlara, A., Hosseini, S. M. H., et al. (2024). Encapsulation of grape seed oil in oil-in-water emulsion using multilayer technology: Investigation of physical stability, physicochemical and oxidative properties of emulsions under the influence of the number of layers. *Current Research in Food Science* 8(February), 100771. <https://doi.org/10.1016/j.crf.2024.100771>
- Silva, E. K., Azevedo, V. M., Cunha, R. L., Hubinger, M. D., & Meireles, M. A. A. (2015). Ultrasound-assisted encapsulation of annatto seed oil: Whey protein isolate versus modified starch. *Food Hydrocolloids*, 56, 71–83. <https://doi.org/10.1016/j.foodhyd.2015.12.006>
- Silva, M., Zisu, B., & Chandrapala, J. (2019). Interfacial and emulsification properties of sono-emulsified grape seed oil emulsions stabilized with milk proteins. *Food Chemistry*, 309, 125758. <https://doi.org/10.1016/j.foodchem.2019.125758>
- Silva, M., Zisu, B., & Chandrapala, J. (2020a). Stability of oil–water primary emulsions stabilised with varying levels of casein and whey proteins affected by high-intensity ultrasound. *International Journal of Food Science and Technology*, 56(2), 897–908. <https://doi.org/10.1111/ijfs.14737>
- Silva, M., Zisu, B., & Chandrapala, J. (2020b). Interfacial and emulsification properties of sono-emulsified grape seed oil emulsions stabilized with milk proteins. *Food Chemistry*, 309(2019), 125758. <https://doi.org/10.1016/j.foodchem.2019.125758>
- Steffe, J. F. (1996). *Rheological Methods in food process engineering* (F. Press, Ed.; 2nd ed.). Freeman Press. [https://doi.org/10.1016/0260-8774\(94\)90090-6](https://doi.org/10.1016/0260-8774(94)90090-6)
- Surini, S., Azzahrah, F. U., & Ramadan, D. (2018). Microencapsulation of grape seed oil (*Vitis vinifera* L.) with gum arabic as a coating polymer by crosslinking emulsification method. *International Journal of Applied Pharmaceutics*, 10(6), 194–198. <https://doi.org/10.22159/IJAP.2018V10I6.24093>
- Taha, A., Ahmed, E., Ismaiel, A., Ashokkumar, M., Xu, X., Pan, S., & Hu, H. (2020). Ultrasonic emulsification: An overview on the preparation of different emulsifiers-stabilized emulsions. *Trends in Food Science and Technology*, 105, 363–377. <https://doi.org/10.1016/j.tifs.2020.09.024>
- Vélez-Eraza, E. M., Bosqui, K., Rabelo, R. S., Kurozawa, L. E., & Hubinger, M. D. (2020). High internal phase emulsions (HIPE) using pea protein and different polysaccharides as stabilizers. *Food Hydrocolloids*, 105. <https://doi.org/10.1016/j.foodhyd.2020.105775>
- Vélez-Eraza, E. M., Carbajal-Sandoval, M. S., Sanchez-Pizarro, A. L., Peña, F., Martínez, P., & Velezmoro, C. (2022). Peruvian Biopolymers (Sapote Gum, Tunta, and Potato Starches) as Suitable Coating Material to Extend the Shelf Life of Bananas. *Food and Bioprocess Technology*, 15(11), 2562–2572. <https://doi.org/10.1007/s11947-022-02902-4>
- Vélez-Eraza, E. M., Consoli, L., & Hubinger, M. D. (2018). Mono and double-layer emulsions of chia oil produced with ultrasound mediation. *Food and Bioprocess Processing*, 112, 108–118. <https://doi.org/10.1016/j.fbp.2018.09.007>
- Wu, J., Guan, X., Wang, C., Ngai, T., & Lin, W. (2022). pH-Responsive Pickering high internal phase emulsions stabilized by Waterborne polyurethane. *Journal of Colloid and Interface Science*, 610, 994–1004. <https://doi.org/10.1016/j.jcis.2021.11.156>
- Yang, C., Shang, K., Lin, C., Wang, C., Shi, X., Wang, H., & Li, H. (2021). Processing technologies, phytochemical constituents, and biological activities of grape seed oil (GSO): A review. *Trends in Food Science & Technology*, 116, 1074–1083. <https://doi.org/10.1016/j.tifs.2021.09.011>
- Yuan, Y., Wan, Z., Yin, S., & Yang, X. (2013). Stability and antimicrobial property of soy protein/chitosan mixed emulsion at acidic condition. *Food & Function*, 4(9), 1394. <https://doi.org/10.1039/c3fo60139k>
- Zhou, L., Zhang, J., Xing, L., & Zhang, W. (2021). Applications and effects of ultrasound assisted emulsification in the production of food emulsions: A review. *Trends in Food Science and Technology*, 110(1), 493–512. <https://doi.org/10.1016/j.tifs.2021.02.008>
- Zhuang, H., Li, X., Wu, S., Wang, B., & Yan, H. (2023). Fabrication of grape seed proanthocyanidin-loaded W/O/W emulsion gels stabilized by polyglycerol polyricinoleate and whey protein isolate with konjac glucomannan: Structure, stability, and in vitro digestion. *Food Chemistry*, 418, 135975. <https://doi.org/10.1016/j.foodchem.2023.135975>